THE HEATSEP METHOD TO MAXIMIZE THE EFFICIENCY OF PUMPED THERMAL ENERGY STORAGE

Sergio Rech[1]*, Piero Danieli[2], Gianluca Carraro[1], Andrea Lazzaretto[1]

[1]University of Padova, Department of Industrial Engineering, Padova, Italy
[2]University of Padova, Department of Management and Engineering, Vicenza, Italy

*Corresponding Author: sergio.rech@unipd.it

ABSTRACT

Storing electricity requires the conversion of the available electrical energy into energy of different form, which can be more easily stored over time. Among the possible options, thermal energy can be generated/accumulated/reconverted using mature technologies that are easy to scale, not constrained by geographic area, and that use safe materials and working fluids. During the charging phase of Pumped Thermal Energy Storage (PTES) the available electricity drives a vapor compression heat pump system (reverse cycle) transferring ("pumping") thermal energy from a cold thermal storage to a hot one. During the discharging phase, a heat engine (direct cycle) uses the thermal energy stored in the hot storage to generate electricity and discharges thermal energy into the cold storage. This paper analyzes all possible configurations of PTES through a multi-objective optimization approach to find the best trade-off between round-trip efficiency and energy density, the latter depending on the specific work of the discharge cycle. The optimization is based on the HEATSEP method, which allows extracting the basic structures of the configurations, named "basic configurations", understood as an assembly of compression and expansion stages and their interconnections. Results shows that the maximum round-trip efficiency of 53% is obtained by a Rankine PTES versus a maximum value of 42% of the Brayton-Joule PTES; energy density shows instead an inverse ranking between Rankine (30 kWh/m^3) and Brayton-Joule (70 kWh/m^3) configuration due to the higher temperatures at which heat can be "pumped" in the latter configuration. Finally, it was found that the little margin for improvement makes not convenient to further complicate the configurations by increasing the number of compression and expansion stages.

KEYWORDS

Pumped Thermal Energy Storage; Multi-Objective Optimization; HEATSEP Method

1 INTRODUCTION

The intrinsic aleatory nature of some RES, together with their unavailability for extended periods (e.g., absence of solar radiation at night, long periods with very low windiness), does not match well with the current energy demands (particularly the electricity one), which are strategically linked to human activities. To enact, without a drastic change in user habits, the transition to an energy system with even increasing shares of renewables needs to adopt proper and massive interventions to "temporally decouple" energy generation from the related consumption. One of the most promising, and currently most realistic, strategies is to integrate Electrical Energy Storages (EESs) within the power grid to make electricity from renewable sources available at later times than when it was generated. In recent years, the trend has been to entrust the function of storing electricity from renewables, in particular on a small and medium scale, to electrochemical storage (batteries) because of their high round-trip efficiency, and fairly high energy density, while neglecting the critical issues related to the use of rare materials, the difficulty in recycling these devices at the end of their life and the significant environmental impact due to their disposal. These issues greatly exacerbated in large-scale use.

https://doi.org/10.52202/077185-0156

Among the solutions for energy storage that are suitable for large scale applications only few are geographically unconstrained and environmentally safe, for these reasons considerable effort has been devoted by researchers worldwide in order to devise different technological options for electrical energy storage. Thermodynamic storage systems, such as Liquid air energy storage (LAES) and Pumped thermal energy storage (PTES) systems, have attracted significant attention in recent years due to several advantages including high energy densities, no geographical constraints and the use of safe materials and working fluids.

During charging phase in LAES systems, electricity is used to drive an air liquefaction process after which liquid air is stored in cryogenic tanks. During discharging phase, pressurized liquid air is re-gasified and expanded through turbomachines to generate electricity. During charging phase in PTES, electricity drives the compressor of a vapor compression heat pump (reverse cycle) transferring ("pumping") thermal energy from a low temperature heat storage device to a high temperature one. During discharging phase, a heat engine (direct cycle) is powered by the heat stored in the high temperature storage device to generate electrical energy, and discharges thermal energy into the low temperature storage device.

This paper focuses on PTES systems and is framed within a broader context of the analysis of storage systems, and it is in addition to the paper by Carraro *et al.* (2023) recently published in which LAES systems configurations presented in the literature are deeply analyzed to identify the criteria behind their conceptual development. The concept of PTES dates back to the work published by Marguerre (1924). In principle every kind of reverse and direct cycle could be used, and any working fluid and storage medium in the low and high temperature storage devices could be selected as long as they are suitable for the range of temperatures in which the system is called upon to operate. In the literature two main categories of PTES systems are proposed: Brayton-Joule PTES, in which the working fluid remains always in supercritical conditions and the storage medium is usually a solid; and Rankine PTES, in which the working fluid undergoes evaporation in the charging phase and condensation in the discharging phase, and the storage medium can be a liquid or a phase change material.

Brayton-Joule PTES was proposed by Desrues *et al.* (2010) and is based on an argon Brayton-Joule cycle with hot and cold solid material storage systems. A PTES system based on a CO_2 transcritical Rankine cycle with hot water and ice-salt slurry as storage medium was patented by ABB Ltd. (Mercangöz *et al.*, 2012) and further developed by Morandin *et al.* (2012). Both PTES types are still under development and an increasing number of papers proposing different configurations are being published.

The different combinations of i) cycle configurations, ii) values of the thermodynamic cycles parameters, e.g., pressures and temperatures, which can vary in a wide range, and iii) choice of working fluid and storage medium, increase the number of possible solutions and make the optimization of the PTES systems very challenging. The literature lacks a comprehensive thermodynamic analysis on these systems and the formulation of a general optimization problem that can consider all their possible configurations. This paper fills this gap and investigates the potential of PTES systems to achieve broad deployment and become competitive in the field of energy storage for large scale applications. The research on this topic is mainly focused on increasing two parameters, which are fundamental to assess performances of an energy storage system:

- *round-trip efficiency*: ratio between the energy extracted from the discharge of the storage and energy consumed to charge the storage in an average charging/discharging process. This must reach a value near today large-scale storage technologies in order to be competitive.
- *energy density per unit volume*: it determines the size of the system given a quantity of energy stored and represents key parameter for judging whether a storage system can be location independent, thus removing the need for specific site characteristics/dimensions. For PTES systems, this parameter depends on both the *specific work* associated with the discharging cycle and the characteristics of the storage medium.

The objective of this work is twofold:

1. analyze the developments of the proposed solutions for PTES systems, in order to understand the general criteria behind the evolution of the systems, and
2. evaluate the maximum performance of PTES systems.

To do this, the advanced optimization method called "HEATSEP" (Lazzaretto and Toffolo, 2008) is applied. This method allows a configuration of any complexity to be reduced into an ordered set of very

https://doi.org/10.52202/077185-0156

limited number of components, named "basic components", that perform the basic processes of the overall system. All possible internal heat transfers of this "basic system configuration" are then optimized. This method is used here to formulate a multi-objective problem that allows finding the best tradeoffs between maximizing round-trip efficiency and maximizing specific work for all basic PTES configurations developed so far. Compared to other methods presented in the literature, the application of the HEATSEP method has the twofold advantage of allowing: i) the identification of the maximum performance practically achievable for each configuration, and ii) the assessment of the maximum margin of improvement achievable by modifying the configuration (e.g. by separating the compression and/or expansion phases into several stages).

2 WORKING PRINCIPLE OF PTES SYSTEMS

Pumped Thermal Energy Storage (PTES) refers to a kind of energy storage system in which energy is stored as thermal energy associated with the temperature difference between the storage mediums contained in one (or more) hot thermal storage and in one (or more) cold thermal storage.
During the charging phase, the available mechanical/electric power moves a heat pump that increases al temperature difference between the hot and cold storages, and therefore the thermal energy stored in the system.
Depending on the working fluid, PTES systems are here subdivided according to the type of direct cycle operated in the discharge phase: when the working fluid remains always in gas phase (e.g., air, argon, CO_2 maintained in the supercritical state) the system is a Brayton-Joule PTES (Figure 1 (a) and (b)), when the operating fluid undergoes condensation during process 8-5 (heat rejection to the cold storage(s)) the system is a Rankine PTES (Figure 1 (c) and (d)). The reverse cycle performed by the heat pump in the charging phase is composed by the following fundamental processes (Figures 1 (a) and (c)):

1-2: compression
2-3: rejecting heat to a sink (hot storage(s))
3-4: expansion
4-1: receiving heat from a source (cold storage(s))

When needed, the thermal energy contained in the system is converted into electricity by means of a direct cycle composed by the following fundamental processes (discharge phase, Figures 1 (b) and (d)):

5-6: compression/pumping
6-7: receiving heat from a source (hot storage(s))
7-8: expansion
8-5: rejecting heat to a sink (cold storage(s))

These processes may be carried out by the same components operating in the charging phase or by other components included exclusively for the discharging phase.
Finally, depending on the storage fluid/medium and the temperatures of the working fluid in the processes 6-7 and 8-5, the thermal energy can be stored in the hot and cold storages as sensible or latent heat.

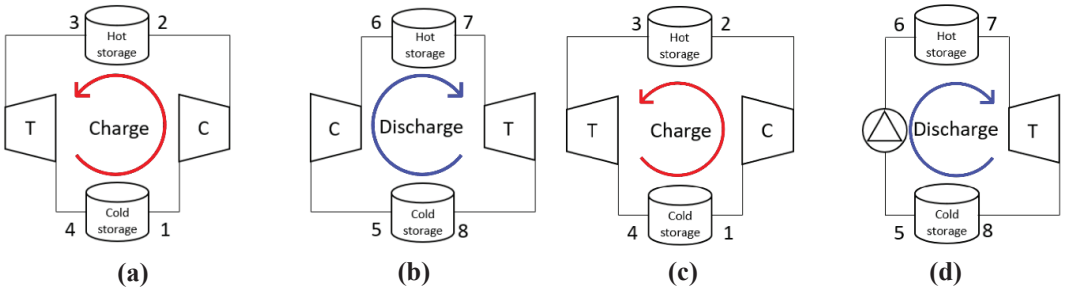

Figure 1: Layout of Bryton-Jule ((a) charging phase, (b) discharging phase) and Rankine ((c) charging phase, (d) discharging phase) PTES systems

https://doi.org/10.52202/077185-0156

3 METHODS

The work starts with a review of the main PTES configurations presented in the literature to understand the evolution of this type of thermodynamic storage system. These configurations are then compared in terms of:

- *Type of thermodynamic cycle in the discharge phase* (Brayton-Joule or Rankine)
- *Working fluid*
- *Number of additional heat exchangers* in addition to any heat exchanger eventually used to store heat in the storage fluid/medium in the storages
- *Characteristics of the thermal storages*: number, type, and storage medium of cold and hot thermal storages
- *Characteristics of turbomachinery*: isentropic efficiency (η_{is}), outlet pressure and temperature (p_{max}, T_{max}) for compressors, outlet temperature for expanders (T_{min}), outlet pressure (p_{max}) and inlet temperature (T_{min}) for pumps, and inlet temperature (T_{max}) for turbines[1]
- *Round-trip efficiency* (Equation (1)), which is defined as the ratio between energy released by the system in the discharge phase (E_{dis}) and the energy used to charge the system (E_{ch}) (based on average charge – discharge process)

$$\eta_{RT} = \frac{E_{dis}}{E_{ch}} \tag{1}$$

- *Energy density per unit volume* (Equation (2)), which is defined as the quantity of energy that can be released by the system per unit of total volume V of the thermal storages (the volume of turbomachinery, piping, and other components is considered as negligible compared with the volume of thermal storages)

$$\varepsilon_V = \frac{E_{dis}}{V} \tag{2}$$

The HEATSEP method by Lazzaretto and Toffolo (2008) is then applied to

i. "Extract" first the so called "basic configurations" from the various configurations, having different complexity, presented in the literature. This method consists of considering the synthesis of the components that perform the internal heat transfers within the system (heat transfer Section) as a separated and subsequent problem than the synthesis of the other components (i.e., compressors, pumps, expanders, components that perform heat exchange with external sources and sinks). These latter "basic components", properly ordered, make up the "basic configuration" and define the main system characteristics. This procedure allows all configurations, regardless of their complexity, to be grouped into a very small number of basic configurations. Note that when considering ideal reversible reverse (charging) and direct (discharging) cycles, the PTES system neither needs to absorb heat from an external source nor release heat to an external sink, i.e., the thermal energy associated with the temperature difference between the hot and cold storages accumulated during charging phase is equal to that required during discharging phase. Thus, no heat exchange performing the absorption/release of heat from/to external sources/sinks is here considered.
   In the real case, considering equal mass flow rate for the two phases, the heat "used" in the discharge phase is always greater than the heat "pumped" in the charge phase due to irreversibilities (see Section 4.1). For simplicity, devices for releasing the excess heat to the external sink (environment) are initially not considered in the basic configuration but added in the final step of defining the heat exchange network.

ii. Optimize all the design parameters of the basic configurations identified in step i., including the internal heat flows, to assess whether there may be room for improvement over the literature results. To this end, the "thermal links" between the basic components are cut to include the

[1] Please note that the variables considered are sufficient to completely define the indirect charge thermodynamic cycle and the direct discharge thermodynamic cycle of the system under the assumption of negligible the pressure drop in the heat exchange devices.

https://doi.org/10.52202/077185-0156

boundary temperatures of all cuts in the set of the decision variables together with the other design parameters (mass flow rates, pressures, temperatures) of the system. In other terms, the configuration of the heat transfer section is not defined in advance but substituted with a black box representing any possible heat transfer within the system. The feasibility of the internal heat transfer is checked in every iteration of the optimization process by building the thermal composite curves at system level as proposed by Kemp (2006).
A multi-objective approach is used to identify the best trade-offs between:

- the maximum of the *round-trip efficiency* defined in Equation (1)
- the maximum *specific work* associated with the direct thermodynamic cycle process (discharging phase) defined as

$$\omega_M = \frac{P_{dis}}{\dot{m}_{WF,dis}} = \frac{W_{dis}}{M_{WF,dis}} = \varepsilon_V \cdot \frac{c_{p,ST}}{c_{p,WF}} \cdot \frac{1}{\rho_{ST}} \tag{3}$$

where P_{dis} is the power generated and $\dot{m}_{WF,dis}$ the mass flow rate of the working fluid in discharging phase; W_{dis} and $M_{WF,dis}$ are the associated work and total mass; $c_{p,ST}$ and $c_{p,WT}$ are the specific heat of the storage medium and working fluid, respectively; and ρ_{ST} is the storage medium density.

Specific work ω_M is chosen as the parameter to be maximized because it depends only on the characteristics of the operating fluid and thermodynamic cycles. When ω_M is known it is possible to calculate the energy density ε_V once the storage medium is chosen (see right side of Equation (3)). To calculate the round-trip efficiency from the only characteristics of thermodynamic cycles it is assumed that the charging and discharging of the system occur simultaneously (with the thermal storage acting as a temporal link between the two sections), as proposed by Carraro *et al.* (2023). The multi-objective design optimization problem of a PTES basic configurations is formulated as

$$\begin{gathered} \text{find } \mathbf{x}^* \in \mathbb{R}^n \text{ that maximizes } \eta_{RT}(\mathbf{x}) \text{ and } \omega_M(\mathbf{x}) \\ \text{subject to } \begin{cases} \mathrm{g}(\mathbf{x}) = 0 \\ \mathrm{l}(\mathbf{x}) > 0 \end{cases} \end{gathered} \tag{4}$$

where $\mathbf{x}$ is the array of the n decision variables (including the boundary temperatures of the thermal cuts), $\mathrm{g}(\mathbf{x})$ and $\mathrm{l}(\mathbf{x})$ are the equations and inequalities of the base configuration model. This model includes mass balances, energy balances, and equations describing the performance of the basic components.

4 RESULTS

4.1 Review and analysis of the literature configurations

Tables 1 and 2 summarize the main characteristics of the literature configurations of Brayton-Joule and Rankine PTES, respectively. All configurations include both hot and cold storages, except the open Brayton-Joule configurations proposed by Guo *et al.* (2016) and Benato (2017), and the Rankine configuration proposed by Steinmann (2013) in which no cold storage is considered and heat in processes 4-1 (charge) and 8-5 (discharge) is exchanged with the environment. The inclusion of the cold storage allows increasing the temperature difference between heat source and heat sink of the direct cycles, and increase its specific work accordingly, regardless of ambient conditions.
In all Brayton-Joule PTES, except the one proposed by Guo *et al.* (2016), thermal storages are composed of a solid thermal medium due to the very low temperature reached by the cold storage (minimum literature value equal to $-166°C$) and the high temperature reached by the hot storage (maximum literature value equal to $995°C$). Temperature difference between hot and cold storage is greater than $700°C$, up to $1000°C$. High temperature differences are necessary to achieve significant system energy density, given the low density of operating fluids. Argon is chosen as working fluid in almost all study, mainly because it is a widely available, inert, nontoxic and has a ratio of the specific heats ($k_{argon} = 1.667$) higher than air ($k_{air} = 1.4$). Accordingly, for lower compression ratios (i.e., fewer compression stages) argon allows obtaining the same compressor outlet temperatures compared to air.

https://doi.org/10.52202/077185-0156

https://doi.org/10.52202/077185-0156

Table 1: Comparison of the characteristics and performance of PTES configurations based on the Brayton-Joule cycle proposed in the literature (SPB = Solid Packed Bed, L = latent, OC = Open Cycle, PT = PolyTropic, n.a. = not available, n.e.d = not enough data to calculate the value)

			Cold storage system		Hot storage system		Charge phase Compressor			Expander		Discharge phase Turbine			
Reference	WF	HE No.	type	N°	type	N°	p_{max} $[bar]$	T_{max} $[K]$	η_{is} $[-]$	T_{min} $[K]$	η_{is} $[-]$	T_{max} $[K]$	η_{is} $[-]$	η_{RT} [%]	$\varepsilon_V = \frac{E_{dis}}{V}$ $[kWh/m^3]$
Desrues *et al.* (2010)	argon	2	SPB (refractory)	1	SPB (refractory)	1	4.60	1268	0.90 (PT)	200	0.90 (PT)	1268	0.90 (PT)	66.7%	27
Howes (2011)	argon	2	SPB (granite)	1	SPB (granite)	1	12.13	773	n.a.	107	n.a.	773	n.a.	72.0%	27
White *et al.* (2013)	argon	2	SPB (gravel)	1	SPB (gravel)	1	10.00	783	0.90 (PT)	123	0.90 (PT)	783	0.90 (PT)	50.0%	26
Ni and Caram (2015)	argon	2	SPB (refractory)	1	SPB (refractory)	1	3.00	773	0.90 (PT)	248	0.90 (PT)	773	0.90 (PT)	65.4%	27
Guo *et al.* (2016)	argon	1	OC	0	L (n.a)	1	n.a.	900	n.a.	n.a.	n.a.	900	n.a.	40.0%	n.e.d.
Benato (2017)	air	1	SPB (various)	1	SPB (various)	1	6.08	823	0.8	203	0.8	823	0.8	9.0%	n.e.d.
Chen *et al.* (2018)	argon	2	SPB (Al_2O_3)	1	SPB (Al_2O_3)	1	4.00	900	0.85	190	0.88	900	0.88	42.0%	n.e.d.
Chen *et al.* (2018)	air	2	SPB (Al_2O_3)	1	SPB (Al_2O_3)	1	4.00	900	0.85	190	0.88	900	0.88	47.7%	n.e.d.
Benato *et al.* (2019)	air	1	OC	0	SPB (various)	1	n.a.	n.a.	n.a.	n.a.	n.a.	1448	n.a.	30.0%	n.e.d.
Wang *et al.* (2021)	helium	2	SPB (n.a.)	1-7	SPB (n.a.)	1-7	10.50	773	0.92	131	0.95	773	0.95	64.9%	31

Table 2: Comparison of the characteristics and performance of PTES configurations based on the Rankine cycle proposed in the literature

			Cold storage system		Hot storage system		Charge phase Compressor			Expander		Discharge phase Pump			Turbine			
Reference	WF	HE No.	type	N°	type	N°	p_{max} $[bar]$	T_{max} $[K]$	η_{is} $[-]$	T_{min} $[K]$	η_{is} $[-]$	p_{max} $[bar]$	T_{min} $[bar]$	η_{is} $[-]$	T_{max} $[K]$	η_{is} $[-]$	η_{RT} [%]	$\varepsilon_V = \frac{E_{dis}}{V}$ $[kWh/m^3]$
Peterson (2011)	propane	1	latent water+glycol	1	sensible granite	1	17.1	340	0.85	258	0.85	17.08	258	0.85	323	0.85	60.0%	4
Mercangöz *et al.* (2012)	CO_2+ ammonia	2	latent ice-salt	1	sensible water	2	140.0	395	0.82	270	0.80	133.1	283	0.80	391	0.86	51.0%	18
Morandin *et al.* (2012,A)	CO_2+ ammonia	6	latent ice-salt	1	sensible water	8	188.7	474	0.86	250	0.85	174.2	254	0.85	450	0.88	60.0%	49
Morandin *et al.* (2012,B)	CO_2	4	latent ice-salt	1	sensible water	6	197.1	454	0.86	250	0.85	165.9	254	0.85	450	0.88	56.4%	44
Morandin *et al.* (2012,B)	CO_2+ ammonia	13	latent ice-salt	1	sensible water	8	146.0	421	0.86	250	0.85	143.3	254	0.85	425	0.88	59.0%	46
Morandin *et al.* (2012,B)	CO_2+ ammonia	5	latent ice-salt	1	sensible water	6	186.4	436	0.86	250	0.85	188.6	254	0.85	440	0.88	48.0%	38
Steinmann (2013)	water	1	ambient	0	latent water	1	n.a.	663	0.90	283	n.a.	n.a.	283	n.a.	643	0.90	70.5%	n.e.d.
Ayachi *et al.* (2016)	CO_2	1	latent ice-salt	1	sensible ground	2	112.3	404	0.85	273	0.90	107	275	0.80	402	0.90	66.0%	n.e.d.
Yan *et al.* (2024)	refrigerants	4	sensible (n.a.)	1	sensible water	2	n.a.	423	0.85	293	0.85	n.a.	298	0.90	423	0.85	72.0%	n.e.d.

Air gives the advantage of an open cycle (Guo *et al.*, 2016; and Benato and Stoppato, 2019), which simplifies the system layout but results in very low values of round-trip efficiency. Finally, helium has been considered by some authors (e.g., Wang *et al.*, 2021) for the higher round-tip efficiency values reachable compared to argon and air, but its significantly higher costs due to greater rarity makes it a worse candidate for large-scale applications.
All the proposed configurations are basically similar, the main difference being the use of an additional electric heater (Ni and Caram, 2015; Benato, 2017; Chen, 2018; and Benato and Stoppato, 2019) to increase maximum temperature or the integration of a bottoming Organic Rankine Cycle (Chen, 2018). Finally, it is worth noting that in all configurations the temperature at the compressor outlet is higher than $400°C$, which is much higher than that reached in current common applications.
Rankine PTES configurations proposed in the literature show instead more substantial differences in their layouts, with the inclusion of various heat exchangers in the effort of increasing internal thermal integration. Moreover, in many cases (Mercangöz *et al.*, 2012; Morandin *et al.*, 2012; Ayachi *et al.*, 2016) an auxiliary cooling cycle is added to store more cooling energy in the cold storage than that provided by principal working fluid. This additional cooling energy is used to cover the difference between the heat absorbed in the reverse cycle (process 4-1 of the charging phase) and the heat released in the direct cycle (process 8-5 of the discharging phase) which is due to the irreversibilities of both cycles. In the other cases (Petterson, 2011, Steimann, 2013 and Ayachi *et al.*, 2016) excess heat is released to the environment. Almost all authors consider a latent cold storage, including water-salt slurry as storage medium, to achieve parallel heat transfer profiles (at constant temperature) in processes 4-1 (charge) and 8-5 (discharge). The most widely used operating fluid is CO_2 because of its natural origin, null ozone depletion potential, non-flammability, no toxicity and favorable thermodynamic properties. In particular, the low critical temperature ($30.98\,°C$) allows a direct transcritical cycle to operate in the discharge phase, which ensures good matching of the temperature profiles in heat transfer (process 6-7) between the operating fluid and sensible storage medium – usually water (Mercangöz *et al.*, 2012). On the other hand, high pressures (above $73.5\ bar$, i.e., the critical pressure of CO_2) are required to operate under transcritical conditions.

4.2 Extraction of the basic configurations

The following "basic configurations" (as defined by the HEASEP method, Toffolo and Lazzaretto, 2008), are extracted from the layouts presented in the literature:

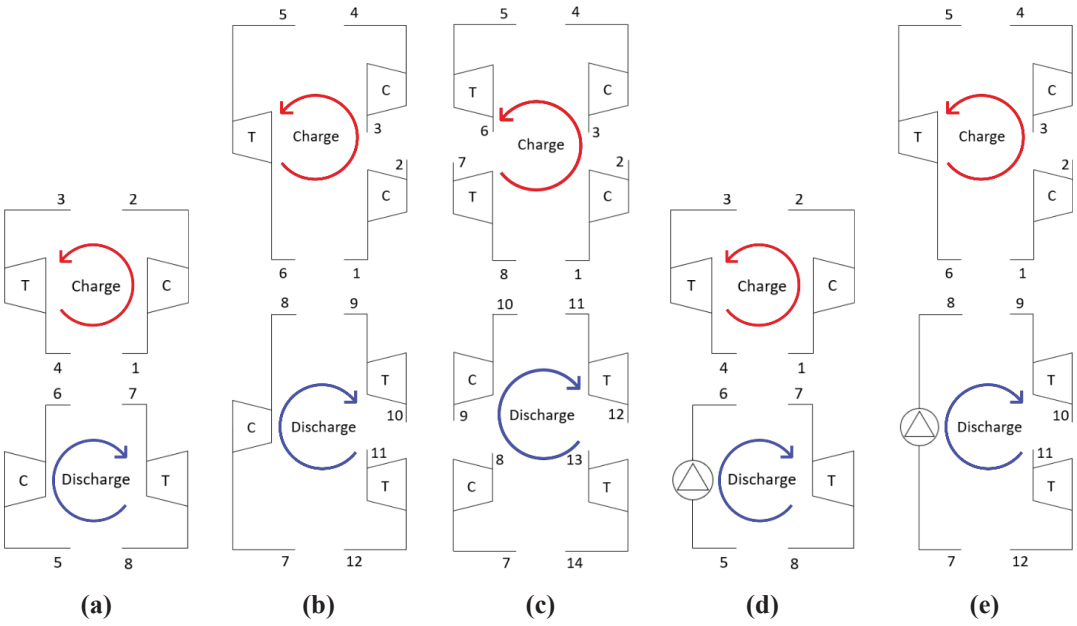

Figure 2: Basic configurations identified for the Brayton-Joule ((a) single stage, (b) half staging, (c) full staging) and the Rankine ((d) single stage, (e) half staging) PTES

https://doi.org/10.52202/077185-0156

1. *Single stage* (Figure 2 (a) and (d)): both the charging and discharging cycle are characterized by only two pressure levels, separated by only a basic pair of components (compressor/turbine or pump/turbine). Two thermal cuts are made in the physical flows connecting the machines
2. *Half staging* (Figure 2 (b) and (e)): the compression process in the charging phase (process 1-2 in Figure 1 (a) and (c)) and the expansion process in the discharge phase (process 7-8 in Figure 1 (b) and (d)) are divided into two stages, in between which a thermal cut is considered
3. *Full staging* (Figure 2 (c)): compression and expansion processes of both charging and discharging phase are divided into two stages interspersed with a thermal link.

The full staging basic configuration (point 3. above) is not considered for the Rankine PTES layout because a significant advantage it is not expected in splitting the pumping process into stages during discharge phase, given the relatively small increase in working fluid temperature in this process.

4.3 Results of the multi-objective optimization

The values of the fixed parameters in design optimization problems of all basic configurations in Figure 2 are listed in Table 3. For the Brayton-Joule PTES a limit of $875\,K$ is imposed on maximum temperatures of the charge cycle (T_2 and T_4) in accordance with the technological limit obtained in the RWE Power EU project "ADELE" (RWE Power, 2010). The variables that are free to vary (decision variables) and their upper and lower bounds are shown in Table 4 for the Brayton-Joule PTES and Table 5 for the Rankine PTES. The working fluid used for Brayton-Joule PTES is argon, the one for Rankine PTES is CO_2.

Table 3: Fixed design parameters assumed in the design optimization problem

Parameter, symbol	Fixed Value
Compressors isentropic efficiency, $\eta_{is,c}$	0.85
Pump isentropic efficiency, $\eta_{is,P}$	0.70
Turbine isentropic efficiency, $\eta_{is,T}$	0.85
Pinch point ΔT in heat exchange	$10\,K$

Table 4: Decision variables and related lower and upper bounds in the optimization problem of the Bryton-Joule PTES configurations (^{S} = single stage, ^{H} = half staging, ^{F} = full staging)

Decision variables, symbol [Unit]	Lower bound	Upper bound
Compressors inlet temperatures (charging phase), $T_1^S, T_3^{H,F}\ [K]$	200	450
Turbine inlet temperatures (charging phase), $T_3^S, T_5^{H,F}, T_7^F\ [K]$	200	450
Compression ratio (charging phase), $\frac{p_2}{p_1}^{S,H,F}, \frac{p_4}{p_3}^{H,F}\ [-]$	3	30
Compression ratio (discharging phase), $\frac{p_7}{p_8}^{S}, \frac{p_9}{p_{10}}^{H}, \frac{p_{11}}{p_{12}}^{H,F}, \frac{p_{13}}{p_{14}}^{F}\ [-]$	3	30

Table 5: Decision variables and related lower and upper bounds in the optimization problem of the Rankine PTES configurations (^{S} = single stage, ^{H} = half staging)

Decision variables, symbol [Unit]	Lower bound	Upper bound
High pressure compressor inlet temperatures (charging phase), $T_3^H\ [K]$	275	300
Turbine inlet temperatures (charging phase), $T_3^S, T_5^H\ [K]$	275	300
Turbine inlet temperatures (discharging phase), $T_7^S, T_9^H\ [K]$	370	450
Low pressure turbine inlet temperatures (discharging phase), $T_{11}^H\ [K]$	275	300
Compressor inlet pressure (charging phase), $p_1^{S,H}\ [bar]$	15	40
Compressor outlet pressure (charging phase), $p_2^{S,H}\ [bar]$	100	200
High pressure compressor outlet pressure (charging phase), $p_4^H\ [bar]$	100	300

https://doi.org/10.52202/077185-0156

The results of the design optimization of the Brayton-Joule basic configurations are shown in Figure 3. Maximum values of round-trip efficiency (η_{RT}) range from 39.5% for single stage layout to 45.1% for full staging layout, while maximum values of specific work (ω_M) range from 89.9 to 198.0 kJ/kg for the same layouts, respectively ($\varepsilon_V = 40$ to $100\ kWh/m^3$ considering titanium oxide as storage medium). Restricting the analysis for simplicity to the single-stage configuration, it is worth noting that the constraint on the maximum value of T_2 (compressor output temperature during charging phase, the maximum value in this analysis is 875 K) represents a limit for maximum system performance. In fact, the optimal solution obtained by excluding this constraint (unlimited maximum temperature) is characterized by the following values of the objective functions, significantly greater than those obtained by considering the constraint: $\eta_{RT} = 52.0\%, \omega_M = 220.0\ kJ/kg$.

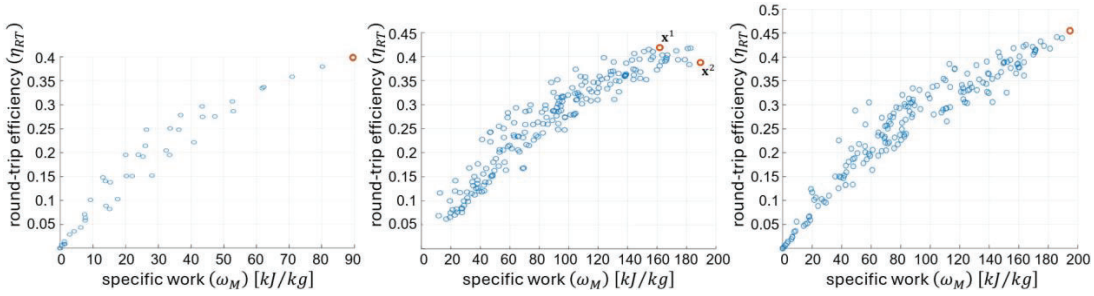

Figure 3: Solutions of the design optimization in the round-trip efficiency and specific workspace for (a) single stage, (b) half staging and (c) full staging Brayton-Joule PTES basic configurations. Orange dots indicate non-dominated solutions (Pareto optimal solutions)

For single stage and full staging layouts, the two objective functions are in agreement with each other throughout the considered search space, and the Pareto front consists of a single solution (Figure 3 (a) and (c)). Conversely, for the half staging layout, the maximum specific work (solution $\mathbf{x}^2$ in Figure 3 (b)) results in a lower round-trip efficiency than the maximum one (solution $\mathbf{x}^1$ in Figure 3 (b)). As an example, the half-stage layout solution corresponding to the highest round-trip efficiency value (solution $\mathbf{x}^1$ in Figure 3 (b)) is characterized by a round-trip efficiency of 42.23% and specific work of $162.97\ kJ/kg$, corresponding to a maximum energy density ε_V of $50.4\ kWh/m^3$ considering titanium oxide as storage medium, and $31.2\ kWh/m^3$ using the more common alumina. This solution requires reaching the temperature limit of 875 K at the outlet of the low-pressure compressor (T_2) during the charging phase (see the thermodynamic cycles in Figure 5 (a)). During this phase, the compression ratio is equal to 6 for the low-pressure compressor (p_2/p_1) and 6.1 for the high-pressure compressor (p_4/p_3), while in the discharging phase the expansion ratios are 3.6 and 3.5 for the high-pressure (p_9/p_{10}) and low-pressure (p_{11}/p_{12}) turbine, respectively. The optimum values of the pressure ratios for all configurations are significantly lower than the upper limit considered in the optimization procedure (30, see Table 4). These values, which are achievable using mature commercial technologies, derives from the best thermal integrations between charging and discharging phases taking into account the binding upper limit on the maximum cycles temperature (875 K).
Figure 4 (a) shows the hot (red) and cold (blue) heat fluxes generated by the optimal values of the temperatures at the edges of the thermal cuts that are listed in Table 6. These heat fluxes, when cumulated, result in the Composite Curves in Figure 5 (b) from which the final configuration (including storages and exchangers) in Figure 4 (b) is built. As introduced in Section 4.1, the cold fluxes are not sufficient to completely compensate the hot ones and it is required to release heat to the environment either during charging (HE S1 and HE S2 in Figure 4 (b)) and discharging (HE S3). The largest amount of heat is released during discharge from the HE S3 exchanger, as highlighted in Figure 5 (b).

https://doi.org/10.52202/077185-0156

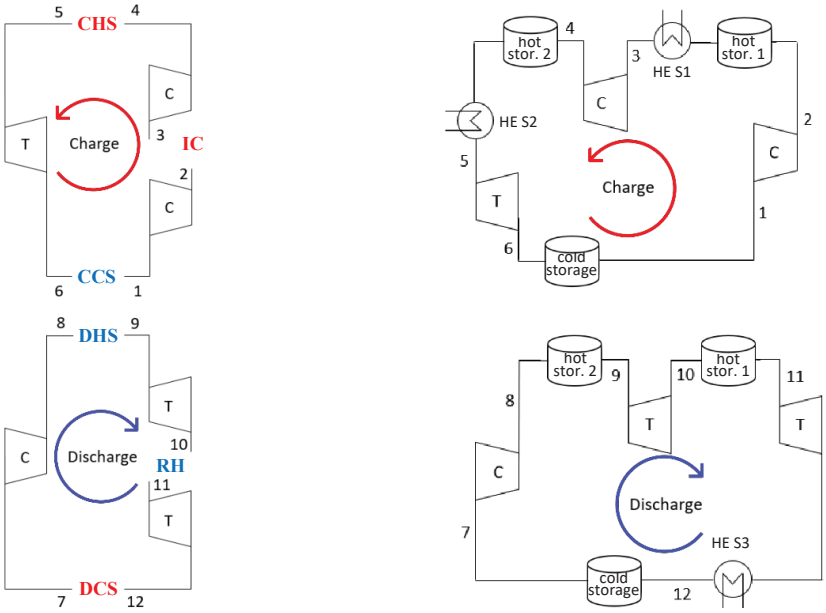

(a) **(b)**

Figure 4: Optimal solution of the half staging Brayton-Joule PTES: (a) basic configuration including names of hot (red) and cold (blue) heat fluxes and (b) final configuration

Table 6: Optimal heat fluxes of the half staging Brayton-Joule PTES layout

	Charging phase			Discharging phase		
	IC	**CHS**	**CCS**	**DHS**	**RH**	**DSC**
T_{in} $[K]$	875.0	773.1	106.4	345.3	505.8	574.0
T_{out} $[K]$	334.5	312.6	378.8	865.94	865.0	116.4

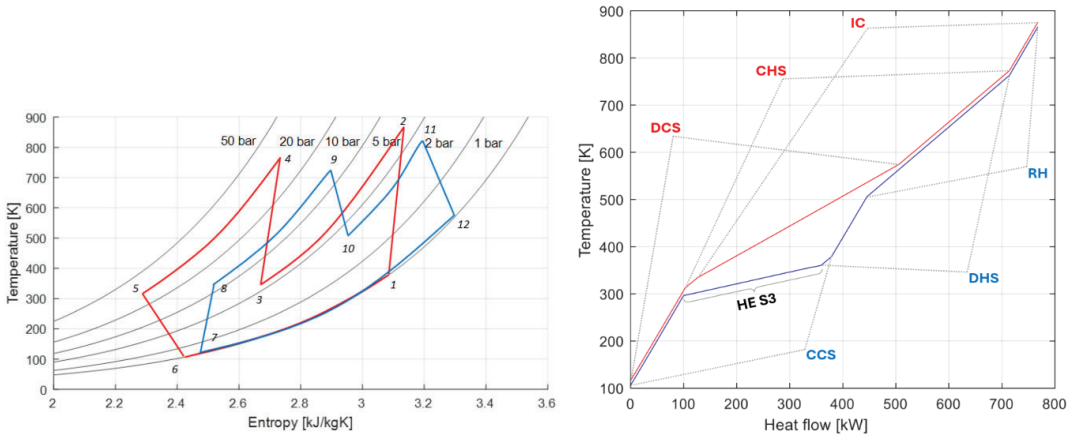

(a) **(b)**

Figure 5: Optimal solution of the half staging Brayton-Joule PTES: (a) reverse (red) and direct (blue) thermodynamic cycles and (b) composite curves

The results of the design optimization of the Rankine basic configurations (Figure 6) clearly show that there is no significant convenience in adopting more complex configurations than the single stage one. The best efficient single stage configuration reaches a round-trip efficiency of 52.50% and a specific work of 68.50 kJ/kg, corresponding to about 30 kWh/m^3 when considering the most common storage

https://doi.org/10.52202/077185-0156

medium. In this solution maximum pressure and temperature in charging (point 2) and discharging (point 7) phase are equal to 131.2 bar at 447.9 K and 151.6 bar at 434.3 K, respectively. Evaporating (charging) and condensing (discharging) pressure are 20.4 bar and 27.4 bar, respectively.

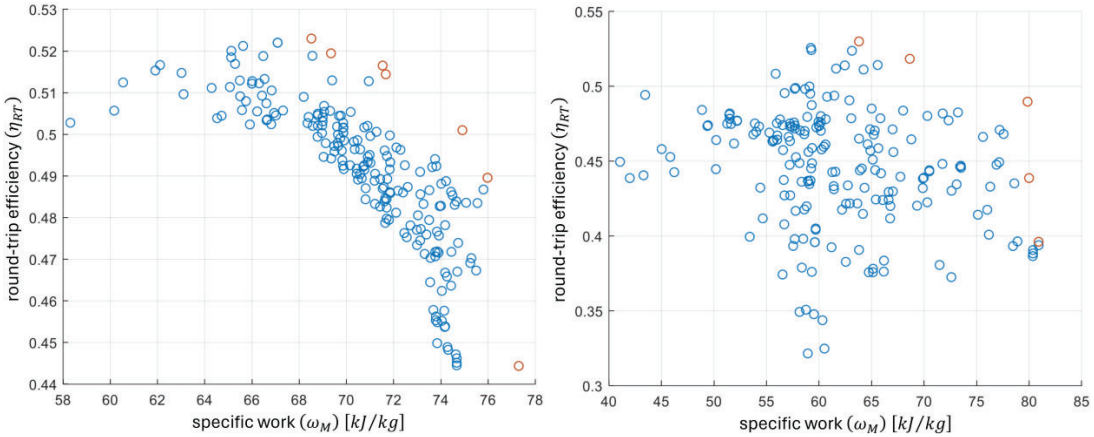

Figure 6: Solutions of the design optimization in the round-trip efficiency and specific work space for the (a) single stage and (b) half staging Rankine PTES

5 CONCLUSIONS

This paper analyzes Pumped Thermal Energy Storage (PTES) systems in terms of configuration, design parameters and maximum achievable performance. Several configurations studied in the literature are first reviewed and critically analyzed. Subsequently, few "basic configurations" are identified starting from all configurations in the literature by using the HEATSEP method, which considers only compressors, pumps and turbines as "basic components" and leaves the temperatures associated with any possible internal heat transfer as decision variables. In this way, each basic configuration is optimized and the maximum achievable values of round-trip efficiency and specific work are obtained. The most efficient ($\eta_{RT} = 53\%$) configuration is the Rankine PTES using CO_2 as working fluid, where the compression in the charging phase and the expansion in the discharge are divided into two stages (half-staging PTES Rankine). However, the simpler single-stage configuration shows only slightly lower performance, with a reduction in round-trip efficiency by 0.5 percentage point while keeping a significant energy density of 30 kWh/m^3 when using a common storage medium. Thus, increasingly complex configurations do not show a performance increase that justifies the higher complexity. This is also confirmed by the analyzed literature configurations in which several complex configurations are less efficient than the basic ones. For these reasons, the only way to achieve substantial performance gains is that of using more efficient machinery and heat exchangers with the storage medium.
Very high values of both energy density and round trip-efficiency are achievable by adopting a Brayton-Joule PTES configuration with no constraints imposed on the maximum temperature at the outlet of the compressors. However, when solutions compatible with the current technological level of components are considered (compressors outlet temperature lower than 875 K) lower levels of round-trip efficiency are obtained than Rankine PTES. Half-staging can partially compensate this limitation associated with maximum temperatures, resulting in a round-trip efficiency slightly higher than 42% and high values of the energy density (up to 50.4 kWh/m^3), while full staging does not show much better performances.

REFERENCES

Ayachi, F., Tauveron, N., Tartière, T., Colasson, S., & Nguyen, D., 2016. Thermo-Electric Energy Storage Based on CO_2 Rankine Cycles and Ground Heat Storage. *Proceedings of the 12th International Conference on Heat Transfer, Fluid Mechanics and Thermodynamics (HEFAT) Conference*.

https://doi.org/10.52202/077185-0156

Benato, A., 2017. Performance and cost evaluation of an innovative Pumped Thermal Electricity Storage power system. *Energy*, vol. 138, 419-436

Benato, A., & Stoppato, A., 2019. Integrated thermal electricity storage system: energetic and cost performance. *Energy conversion and management*, vol. 197, 111833.

Carraro, G., Danieli, P., Boatto, T., & Lazzaretto, A., 2023. Conceptual review and optimization of liquid air energy storage system configurations for large scale energy storage. *Journal of Energy Storage*, vol. 72, Part B, 108225

Chen, L. X., Hu, P., Zhao, P. P., Xie, M. N., & Wang, F. X., 2018. Thermodynamic analysis of a High Temperature Pumped Thermal Electricity Storage (HT-PTES) integrated with a parallel organic Rankine cycle (ORC). *Energy conversion and management*, 177, 150-160

Desrues, T., Ruer, J., Marty, P., & Fourmigué, J. F., 2010. A thermal energy storage process for large scale electric applications. *Applied Thermal Engineering*, vol. 30, no. 5, 425-432

Guo, J., Cai, L., Chen, J., & Zhou, Y., 2016. Performance evaluation and parametric choice criteria of a Brayton pumped thermal electricity storage system. *Energy*, vol. 113, 693-701

Howes, J., 2011. Concept and development of a pumped heat electricity storage device. *Proceedings of the IEEE*, vol. 100, no. 2, 493-503

Kemp, I. C. (2006). Pinch analysis and process integration: a user guide on process integration for the efficient use of energy, https://doi.org/10.1016/B978-0-7506-8260-2.X5001-9

Lazzaretto, A., & Toffolo, A., 2008. A method to separate the problem of heat transfer interactions in the synthesis of thermal systems. *Energy*, vol. 33, no. 2, 163-170

Marguerre, F., 1924. Ueber ein neues Verfahren zur Aufspeicherung elektrischer Energie. *Mitteilungen der Vereinigung der Elektrizitätswerke*, vol. 354, no. 55, 27-35

Mercangöz, M., Hemrle, J., Kaufmann, L., Z'Graggen, A., & Ohler, C., 2012. Electrothermal energy storage with transcritical CO_2 cycles. *Energy*, vol. 45, no. 1, 407-415

Morandin, M., Maréchal, F., Mercangöz, M., & Buchter, F., 2012. Conceptual design of a thermo-electrical energy storage system based on heat integration of thermodynamic cycles–Part A: Methodology and base case. *Energy*, vol. 45, no. 1, 375-385

Morandin, M., Maréchal, F., Mercangöz, M., & Buchter, F., 2012. Conceptual design of a thermo-electrical energy storage system based on heat integration of thermodynamic cycles–Part B: Alternative system configurations. *Energy*, vol. 45, no. 1, 386-396

Ni, F., & Caram, H. S., 2015. Analysis of pumped heat electricity storage process using exponential matrix solutions. *Applied Thermal Engineering*, vol. 84, 34-44

Peterson, R. B., 2011. A concept for storing utility-scale electrical energy in the form of latent heat. *Energy*, vol 36, no. 10, 6098-6109

RWE Power, 2010. Adele–adiabatic compressed-air energy storage for electricity supply. *RWE Power AG*, Essen/Koln, 141.

Steinmann, W. D., 2013. Thermo-Mechanical Storage of Electricity at Power Plant Scale. *Energy Sustainability*, vol. 55515, p. V001T09A002

Wang, L., Lin, X., Zhang, H., Peng, L., & Chen, H., 2021. Brayton-cycle-based pumped heat electricity storage with innovative operation mode of thermal energy storage array. *Applied Energy*, vol. 291, 116821.

White, A., Parks, G., & Markides, C. N., 2013. Thermodynamic analysis of pumped thermal electricity storage. *Applied Thermal Engineering*, vol. 53, no. 2, 291-298.

Yan, Y., Yang, F., Zhang, H., Yu, M., Ping, X., Pan, Y., ... & Li, J., 2024. Thermodynamic evaluation of a novel Rankine-based pumped thermal energy storage concept targeting thermal coordination and large temperature span. *Energy Conversion and Management*, vol. 309, 118439.

ACKNOWLEDGEMENT

Eng. Tazio Boatto (ATG Europe) are gratefully acknowledged for the support in model development and calculations.

https://doi.org/10.52202/077185-0156